Rev. Roum. Sci. Techn.– Électrotechn. et Énerg.
Vol. **69**, *1*, pp. 67–72, Bucarest, 2024

EXPERIMENTAL ANALYSIS OF POWER SEMICONDUCTOR ELEMENTS USED IN FLYBACK CONVERTERS

OVIDIU LĂUDATU, DRAGOS NICULAE, MIHAI IORDACHE, MARIA-LAVINIA BOBARU, MARILENA STĂNCULESCU

Keywords: Switch-mode power supply; Flyback; MOSFET; IGBT; Fast recovery diode; Schottky diode.

Switch-mode power supplies (SMPS) have become very popular lately due to their superior efficiency and compact dimensions as compared to conventional counterparts which contain low-frequency transformers. This efficiency and miniaturization are connected to several factors, including high operating frequencies typically in the kHz to MHz range, the utilization of ferromagnetic materials for inductive coupling, and the incorporation of active switching components to mitigate energy loss via the Joule-Lenz effect. Enhancing SMPS efficiency implies active circuit elements (diodes, transistors, etc.) sizing and arrangements. This paper presents a practical approach by addressing a series of experiments to analyze and compare the performance of different active components. It starts with the analysis of the PWM generator module from the primary and continues with the field-effect transistors and rectifier diodes in the secondary. The asynchronous flyback topology has been chosen to carry out the experiments. By using the same experimental platform, based on the obtained results, the analysis of behavioral differences between the different components has been performed.

1. INTRODUCTION

Switch-mode power supplies (SMPS) are integral electronic modules extensively used in modern electronics. They need to be continuously improved to ensure the best possible efficiency for the required electrical parameters and for other parameters such as: minimum size, reduced electromagnetic interference (EMI) emissions, etc. Using a practical approach, the main scope of this article is to analyze and conclude which components are more suitable for a SMPS with flyback topology, such that the efficiency of the power supply to be maximum.

In general, flyback converters are chosen for low power applications, for which the loads must be isolated from ac supply. Unlike the buck-boost converter, the flyback topology provides galvanic separation [1,9] between the module in the primary. In the primary, the module is supplied by a high voltage level, and the module in the secondary the output voltage has a lower value. This topology offers the advantage of having large voltage differences between the module in the primary and the module in the secondary. This is due to the transformation ratio K of the transformer because the active elements of the circuit can be sized to work efficiently. The experimental module uses the asynchronous flyback configuration, which means that the rectifier module in the secondary is not controlled by a driver circuit. It only rectifies semi-alternating currents when the diode or transistor is directly biased. In this paper, by using the same experimental platform we managed to analyze the difference between the MOSFET transistor and the IGBT transistor. In addition, we analyzed the differences in conductance between an ultra-fast diode, a Schottky diode, and a MOSFET transistor used in rectification mode.

The experimental set-up has been designed to ensure the best accuracy of the experimental values. We considered the measurements corresponding to the controlled elements (transistors), and for the non-controlled elements (diodes and non-controlled transistor operating in rectifier mode). The experimental measurements took place using a RIGOL DS1054Z oscilloscope, having calibrated probes. To avoid the interaction between the grounding of the oscilloscope and the switching power supply, a galvanic isolation transformer was used to power the oscilloscope.

2. ACTIVE CIRCUIT ELEMENTS

Literature [1–8] reports a wide range of semiconductor elements used in the construction of switching power supplies (Fig. 1). To increase the efficiency of the active circuit power elements, we chose the components commonly used in the construction of power supplies using flyback [9] topology.

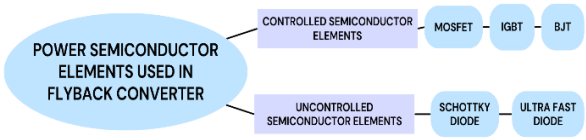

Fig. 1 – Active circuit elements used in SMPS.

Modulation of the current in the primary winding is done with BJT, MOSFET or IGBT transistors. MOSFET and IGBT transistors are voltage-controlled circuit elements, and simulation using the same electronic circuit is not possible for BJT transistor, which is current-controlled.

2.1. INSULATED-GATE BIPOLAR TRANSISTOR

The experiments were carried out only on MOSFET and IGBT. The bipolar transistor sends similar parameters to the IGBT transistor, considering it controls a BJT transistor (Fig. 2). The IGBT transistor can be defined as a voltage controlled BJT transistor. It mainly consists of a field effect transistor and a BJT transistor. The main current flows through the BJT-PNP transistor, which is polarized by a field effect transistor. The last one is controlled from the outside, and consequently its grid is accessible.

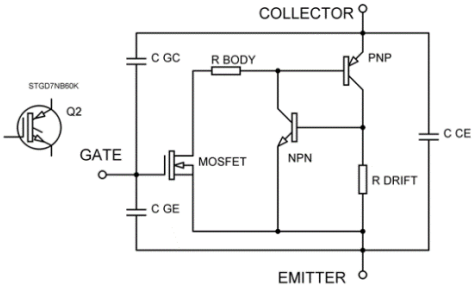

Fig. 2 – Internal electronic diagram of an IGBT.

Faculty of Electrical Engineering, National University of Science and Technology "Politehnica" of Bucharest, Romania
E-mails: ovidiu.laudatu@stud.electro.upb.ro, dragos.niculae@upb.ro, mihai.iordache@upb.ro, lavinia.bobaru@upb.ro, marilena.stanculescu@upb.ro

DOI: 10.59277/RRST-EE.2024.69.1.12

R body (Fig. 2) limits the control current of the PNP transistor. This limitation is necessary for the inductive loads case (*e.g.* the primary winding of the transformer).

To increase the efficiency of the IGBT transistor under high variable loads, R drift and the NPN transistor [7] provide better biasing of the PNP transistor. Due to the absence of minority carrier transport, MOSFET can be operated at higher frequencies in comparison with the IGBT. The limit is given by the transit time of electrons across the drift area and the charge-discharge time of the gate and of the Miller-capacitance. IGBT operates like a MOSFET with an injecting region on its collector [2].

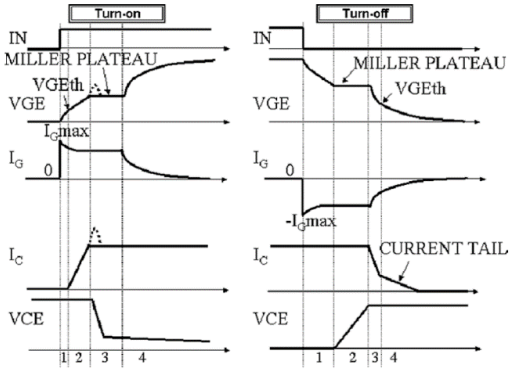

Fig. 3 – IGBT on and off state [3].

The input of IGBT transistor in conduction mode and off mode are given in the simulation from Fig. 3 [3] where: VGE – the emitter grid voltage; VGEth – the minimum threshold bias voltage; Miller plateau – the transistor enters conduction; Vge maintains its value, due to CGC (Fig. 2); I_G – grid current; $I_G$max – high initial current due to high switching frequency and small CGS reactance (Fig. 2); I_C – collector current, VCE – emitter-collector voltage.

2.2. MOSFET TRANSISTOR

The control circuit of a MOSFET transistor, as well as its parasitic capacitances, are illustrated in Fig. 4.

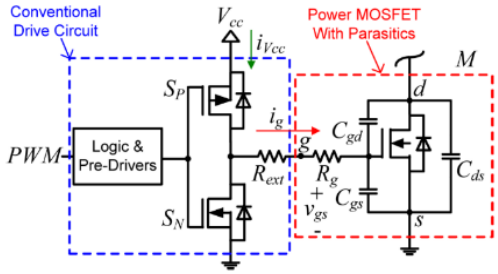

Fig. 4 – Conventional gate drive circuit with power MOSFET and its associated parasitic [4].

For the conventional driver, the gate energy loss due to charging and discharging the gate capacitance of M is given by (1), where Q_g represents the total gate charge, V_{cc} is the driving voltage and f_s is the switching frequency[4,2]:

$$\mathrm{Pg} = \mathrm{Q_g} * \mathrm{Vcc} * fs(W)\ . \quad (1)$$

The gate energy is dissipated as RMS loss in:

1) the driver switches S_N and S_P
2) the external resistance, R_{ext}
3) the MOSFET internal gate mesh resistance of M. This loss component is well understood and is often called the CV^2 gateloss. In addition to the CV^2 loss, conventional gate drivers exhibit switching loss, shoot-through loss and gate loss in their switches [4].

The MOSFET transistor, unlike the IGBT, operates at a higher frequency; for this reason, more attention must be paid to the transition regimes between conduction and blocking (Fig. 5).

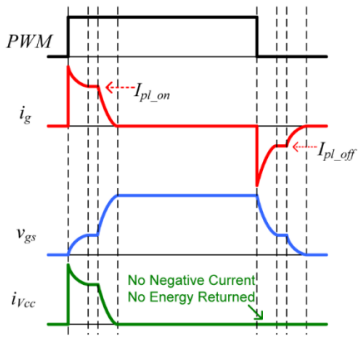

Fig. 5 – Power MOSFET gate drive waveforms-conventional gate drive [4].

For better switching efficiency, Ton and Toff times should be as small as possible. In Fig. 5, we can see the two transitions, PWM represents the input signal, I_g – represents the current through the transistor, V_{gs} – the gate-source voltage, I_{Vcc} – the current through the driver module of the MOSFET transistor.

No negative current and no energy returned, because at the Toff moment the stored charge C_{gs} is dissipated by the impedance to GND created by S_n through R_{ext} and R_g.

During the turn on switching time from the threshold to the end of the Miller plateau, the gate current decays to I_{pl_on}. During the turn off switching time, the problem is even more severe since the gate current decays to I_{pl_off}.

The on-state resistance RDS(on) of a MOSFET is consists of following resistances [2]: R_{source} – source resistance; R_{ch} – channel resistance; RA – accumulation resistance; RJ – two body regions resistance; RD – drift region resistance; R_{sub} – substrate resistance and the corresponding relationship between them is given below [2]:

$$\mathrm{RDS(on)} = R_{source} + R_{ch} + \mathrm{RA} + \mathrm{RJ} + \mathrm{RD} + R_{sub}\ . \quad (2)$$

The information of the collector-emitter resistance of a IGBT opposite the MOSFET [6] with comparable blocking capabilities can be expressed as follows [2]:

$$\mathrm{RCEon\ (IGBT)} = \frac{1}{6\text{–}10}\ \mathrm{RDSon(MOSFET)}\ . \quad (3)$$

Gate-source capacitor C_{GS}do not depend on the applied voltage and is the resulted capacitance due to the overlap of the source and the channel regions around the gate.

Gate-drain capacitor C_{GD} consists of two parts:

– the capacitance between the gate and the capacitance underneath in the JFET region;

– the capacitance associated with the depletion region immediately under the gate site.

Drain-source capacitor C_{DS} is the capacitance associated with the integrated body-drift diode. This value is a function of the drain-source bias. The on-state voltage VDS (on) of the available MOSFETs is higher for MOSFETs than for comparable bipolar components [2–4].

2.3. RECTIFIER DIODES

Switching power sources are defined as asynchronous, if there is no controlled rectifier element in the secondary, and synchronous, if there is a controlled voltage rectifier element.

The experiments took place using an asynchronous flyback converter. The rectifier elements used are ultra-fast

diode (Si-diode), Schottky diode, and MOSFET transistor (polarized by the transformer's output voltage).

A significant part of the overall losses of Si-based power converter are the reverse-recovery switching losses of Si diodes [5]. The reverse recovery of Si diodes affects the primary transistor causing additional turn-on losses and leads to a significant amount of noise in the system [5].

3. EXPERIMENTAL FLYBACK CIRCUITS

To analyze the behavior of semiconductor electronic components, using Proteus program, we designed a flyback power supply able to work with both MOSFET and IGBT transistors in the primary module. To be able to use different rectifier elements and to use the same switching power supply with flyback topology, the solution was to have a common configuration in the secondary module.

The power supply uses a common controller from the UC3843 series. This is a PWM controller, where the gate pulses are current-controlled. The output power of the source is small, this configuration being used to power different pieces of equipment such as: laptops, phones, desktops, monitors. The model ensures galvanic separation, operating in closed-loop mode (closes the reaction loop through an optoisolator). The main parameters of the power supply can be seen in Table 1.

Table 1

Flyback converter parameters

Parameters	*Values*
rated power(W)	18
AC rated input voltage (V)	80-250
DC rated output voltage (V)	12
Switching frequency (kHz)	40
Output current (A)	1.5
PWM control signal max dt. (%)	95

The experiments took place for average load conditions: the load connected to the output is a resistor and the delivered power was 4.36 W.

3.1. EXPERIMENTAL IGBT CIRCUIT

Figure 6 presents the electronic diagram of the flyback converter when the primary winding current is controlled by an IGBT transistor (Fig. 2). The gate is controlled by UC8343, through a totem-pole driver circuit, composed of two bipolar transistors. R1 limits the control current, ensuring better switching; its value is 10 Ω for all proposed circuits to be tested. The IGBT transistor used is STGD7NB60K.

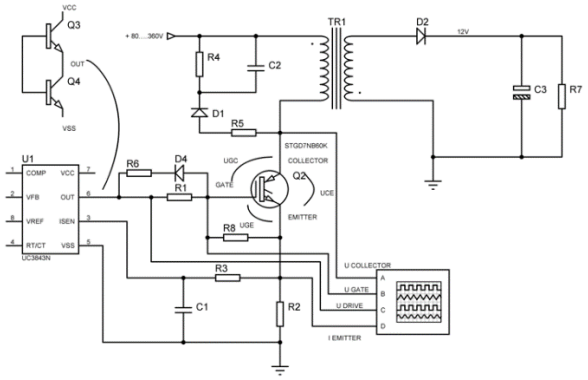

Fig. 6 – Flyback converter using IGBT in the primary.

Functioning description (Fig. 7): Diode D4 and resistor R6 ensure a faster discharge of the C_{GE} (Fig. 2)) loads, during the transition to Toff.

R6 provides a discharge of the charges initially stored by the C_{GE} and C_{GC} (Fig. 2). The group R4, R5, C2, D1 represents the snubber circuit, R4 discharges the charges stored in C2, D1 ensures unidirectional conduction [8], and R5 limits the current spikes that occur when D2 turns on.

These spikes appear due to the low capacitive reactance of the capacitor at the time of charging. Thus, the resulting circuit attenuates the high frequency variations appearing in the switching node. The oscillator circuit in the primary controls the pulses through the IE current, and attenuate the unwanted high frequencies, R3 and C1 form a low-pass filter, which provides a ramp of the current with alternative high-frequency components, drastically attenuated.

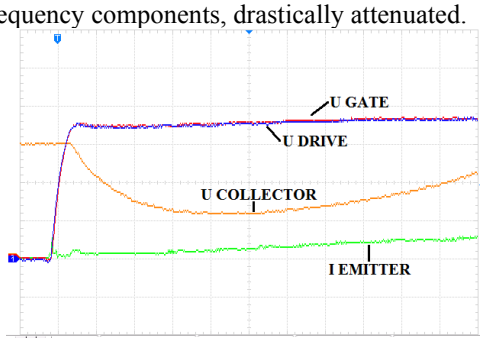

Fig. 7 – Waveforms at the time the IGBT transistor turns on.

Analyzing the waveform from Fig.7, the value of the collector-emitter voltage amplitude u does not reach almost zero, which means that the PNP bipolar transistor (fig. 2) is not polarized correctly. This is due to the very small value of the current through the primary winding. To calculate the value of the bias current of the IGBT transistor, we use the following formula:

$$\text{I GATE} = \frac{\text{U DRIVE} - \text{U GATE}}{\text{R1}} \text{ (A)} \quad . \tag{4}$$

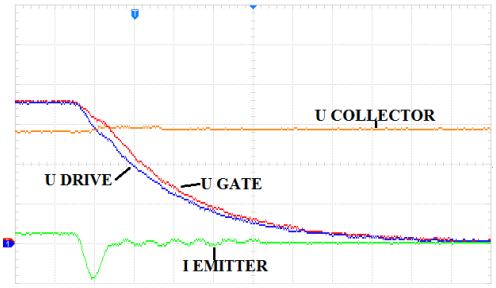

Fig. 8 – Waveforms at the time the IGBT transistor turns off.

The value of the emitter current can be seen in Fig. 8. In addition, that negative current spike is due to the control pulse in the grid, and the collector-emitter voltage is maintained at a high value.

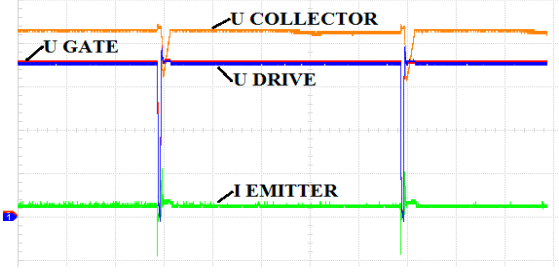

Fig. 9 – Waveforms at the time the IGBT transistor turns on and off.

The time needed by the transistor IGBT to enter a conduction state is very small compared to the time needed to enter blocking state. As a conclusion, to properly drive a IGBT transistor, this must be biased with a negative grid voltage. Under these conditions, the power source works but its efficiency is very low due to the large voltage drops emitter-collector. Figure 9 shows the turn-on and turn-off times of the IGBT transistor. In this case, the feedback loop tries to compensate for the losses caused by incorrect biasing of the transistor, which operates at maximum duty cycle.

3.2. EXPERIMENTAL MOSFET CIRCUIT

Figure10 presents the diagram of the converter (similar to the one from Fig. 6), but IGBT transistor has been replaced by a MOSFET. This will allow the comparison of the behaviors of the two switching elements. The MOSFET transistor used is STP6NC60.

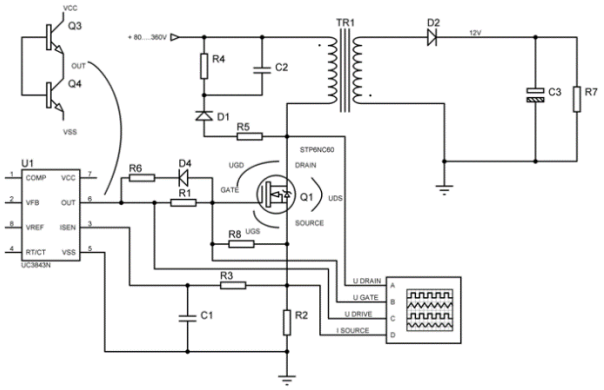

Fig. 10 – Flyback converter using MOSFET in the primary.

The above configuration is commonly used in power supplies using flyback topology. When the transistor has a very high drain-source voltage (OFF time) the voltage drop U_{DS} can be calculated using $RDS_{(on)}$ from equation 2. The same formula (eq.4) applies for the calculation of the input current in the IGate, R1-10Ω.

Analyzing the waveforms presented in Fig. 11, we can see that the Gate voltage slope is increasing until the U_{th} moment, then the transistor enters conduction and the current decreases (Miller Plateau) due to the inductive load in the I_{DRAIN}.

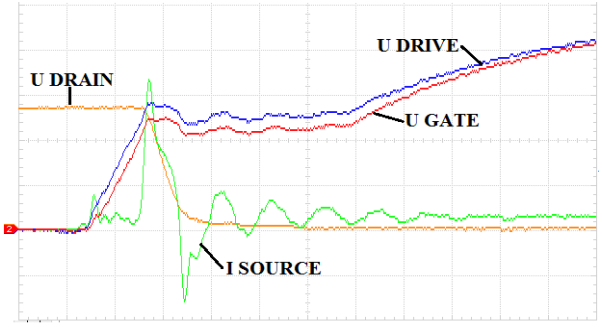

Fig. 11 – Waveforms at the time the MOSFET transistor turns on.

Even if, after entering the conduction mode, the voltage in the GATE maintains its value for a short period of time and the I_{SOURCE} current presents a short high-frequency oscillation, the U_{DS} voltage is not affected. Therefore, it results a correct polarization of the MOSFET transistor.

The transistor MOSFET from Fig. 11 has a higher turn-on time compared to the IGBT transistor in Fig. 7.

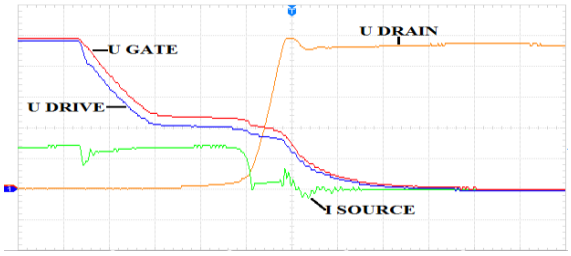

Fig. 12 – Waveforms at the time the MOSFET transistor turns off.

The entry into blocking mode of the MOSFET transistor is presented in Fig. 12, where I_{SOURCE} represents the current from the source. Two green current spikes that control the polarization of the GATE. Can be observed. Due to $RDS_{(on)}$ low conduction mode, the voltage drop in the U_{DRAIN} line is very small.

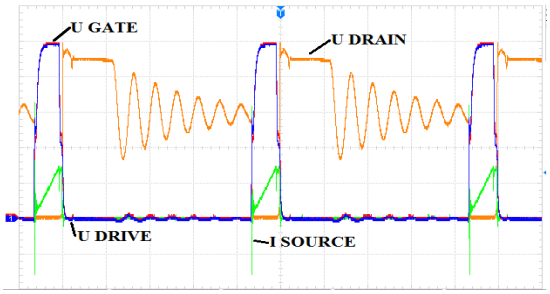

Fig. 13 – Waveforms at the time the MOSFET transistor turns on and off.

In Fig. 13, both on and off periods of the transistor can be observed. To compare the differences in operation between an ultra-fast diode, a Schottky diode and a MOSFET transistor operating in rectifier diode mode, three experimental modules have been developed. Their presentations are given in next sections.

3.3. EXPERIMENTAL ULTRA FAST DIODE CIRCUIT

The experimental circuit Fig. 14 uses a flyback topology asynchronous switching power supply. The rectifier diode in the secondary module is an ultra-fast diode UF5408.

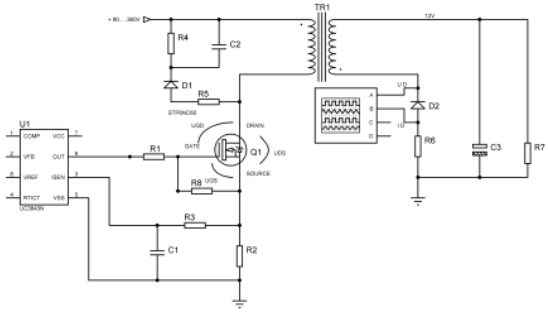

Fig. 14 – Flyback converter using ultra-fast diode in the secondary.

The module in the primary uses the UC3843 circuit and the MOSFET transistor to control the current in the primary winding.

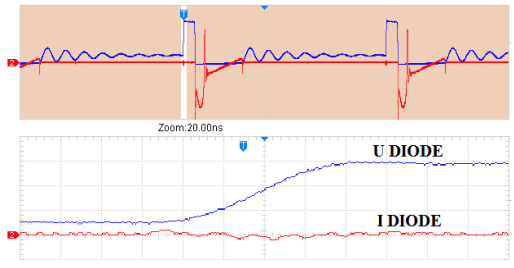

Fig. 15 – Waveforms of the ultra-fast diode UF5408, in blocking mode.

In Fig. 15, the ultra-fast diode is in blocking mode. This is the moment when the transistor enters blocking mode. All this time the current through the diode is very close to 0A.Its small oscillations are due to the parasitic capacitance of the diode. UF5408 has 36pF typical junction capacitance.

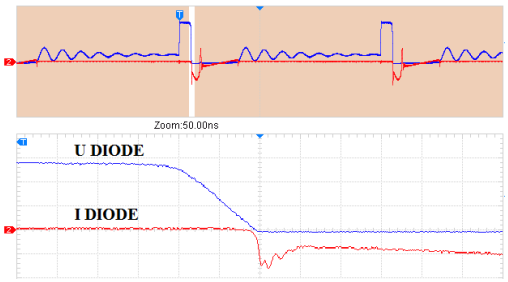

Fig. 16 – Waveforms of the ultra-fast diode UF5408, conduction mode.

In Fig. 16 the ultra-fast diode enters conduction mode, with a corresponding period of approximately 120ns. The voltage drop across the conducting diode for a current of 0.5 A is about 0.6 V. The current was measured using resistor R6 having a value of 0.1 Ω. Resistor load R7 connected to the output has a value of 33 Ω, output voltage is 12 V. The advantage of an ultra-fast diode over a Schottky diode is that it provides a very high reverse bias voltage, but a higher voltage drop when operating in forward bias mode.

3.4. EXPERIMENTAL SCHOTTKY DIODE CIRCUIT

Using the same experimental platform, a Schottky diode has been connected in the secondary module to rectify the voltage. Like the circuit in Fig. 14, we analyzed the voltage drop on the diode and the current. We used a resistor R6 with a value of 0.1Ω to measure the current.

The Schottky diode supports high frequencies and very high currents. The disadvantage of this diode is the reverse bias voltage, which is very small compared to the other diodes working in the same frequency range and high typical junction capacitance of 250 pF(SB3100).

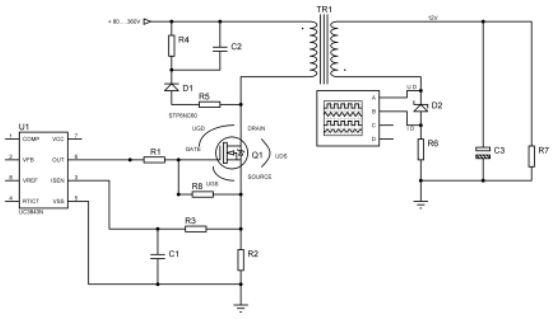

Fig. 17 – Flyback converter using Schottky diode SB3100 in the secondary.

For this reason, it is usually used in step-down power supplies. Figure 17 presents the switching power supply with a Schottky rectifier diode in series with a shunt resistor in the secondary module.

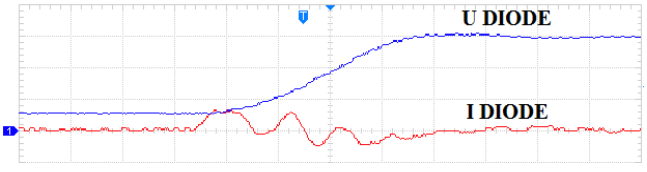

Fig. 18 – Waveforms of the Schottky diode SB3100, being in blocking mode.

Analyzing the waveforms presented in Fig. 18, we can see the diode in the blocking mode due to the very high parasitic capacitance. The current through the diode has high frequency oscillations. Compared to the oscillations in Fig.15 using the ultra-fast diode, the Schottky diode in Fig. 18 shows oscillation with a larger amplitude in blocking mode.

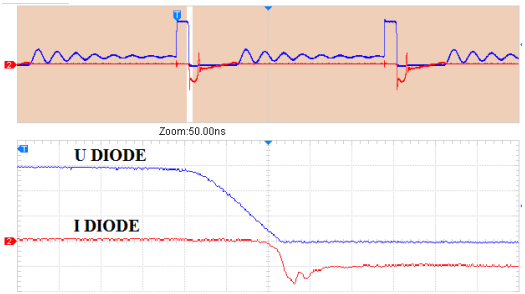

Fig. 19 – Waveforms of the Schottky diode SB3100, in conduction mode.

The entry into conduction of the Schottky diode can be analyzed in Fig. 19. We can see a small delay of the current versus the voltage. This delay is bigger than in the case of the ultra-fast diode. The voltage drop across the conducting diode is much lower compared to the ultra-fast diode which makes it more efficient in conducting mode.

3.5. EXPERIMENTAL MOSFET RECTIFIER CIRCUIT

A more efficient way to rectify the voltage in the secondary is to use a field-effect transistor to limit the voltage drop on the conducting semi-conductor element as much as possible. The voltage drop in this case is given by the resistance $RDS_{(ON)}$ (2) .

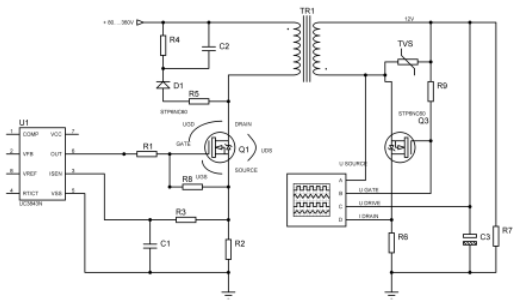

Fig. 20 – Flyback converter using MOSFET rectifier in the secondary.

The experimental set-up Fig. 20 contains a MOSFET transistor in the secondary. In this case, it must be biased directly by the output voltage from the secondary winding of the transformer without the need for a transistor control circuit itself. However, we must consider that it is an inductive load and there are voltage spikes. So, we must connect a circuit or a signal amplitude limiting component, such as to limit the maximum bias voltage and not to destroy the rectifier element. The transistor used is STP6NC60 it allows a maximum U_{GS} voltage of 20V.

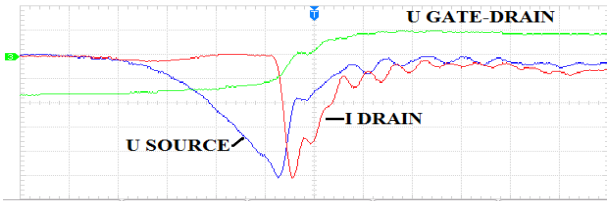

Fig. 21 – Waveforms of the flyback converter using MOSFET rectifier in the secondary, transition mode.

In Fig. 21 we can see the waveforms of the transistor connected in the secondary operating in the rectifier diode mode and the current which can be established such that the circuit to be functional. Due to the inductive behavior of the bias voltage of the transistor the current does not have a linear characteristic. In conclusion, a separate circuit is required to control the transistor for the best possible rectification efficiency.

A special control circuit is required from the measured waveforms to maintain the bias voltage when the transistor is in conduction mode without oscillating voltages appearing in the gate control.

4. EXPERIMENTAL SETUP AND INTERPRETATION OF THE RESULTS

Figure 23 presents the laboratory experimental module containing the oscilloscope and the flyback power supply module. The tests and data acquisition presented in the previous sections have been performed in this module.

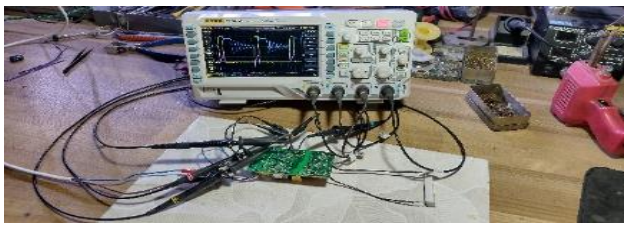

Fig. 23 – Laboratory setup of the experimental flyback board.

We analyzed five configurations of power semiconductor elements. Based on the measured values from the proposed set-ups, valuable conclusions are related to the components connected to the primary module and to the rectifier semiconductor components used in the secondary module. In the first two experimental modules, we analyzed which of the two transistors are more suitable for a flyback switching power supply commonly used with a maximum power of 50 W. Both transistors offer advantages and disadvantages. From the results obtained, we conclude the MOSFET transistor is more suitable because it works more efficiently than the IGBT. In addition, the MOSFET transistor offers a lower source-drain voltage drop due to the $R_{DS(on)}$ resistance. This makes it more efficient than the IGBT, which has a higher collector-emitter voltage drop at low collector currents.

Three experiments were used to compare an ultra-fast diode, a Schottky diode, and a MOSFET transistor. All these components are used in rectification mode in the secondary module of a flyback switching power supply. If the power supply operates in a voltage-lowering regime (230 V to 12 V) in the secondary, the optimal choice is the Schottky diode. Schottky diode is better because it offers a lower conduction voltage drop than the ultra-fast diode. Even if the parasitic capacitance of the diode is higher than that of an ultra-fast diode (pF range), this does not represent a significant loss of energy operating in the kHz frequency range. If the power supply is a step-up one, then the optimal choice would be an ultra-fast diode because it allows a high reverse bias voltage. Regarding the rectification using a MOSFET transistor without a control circuit, the voltage presents fluctuations due to the inductive nature of the transformer. The transistor enters an instability regime, which makes it less efficient.

5. CONCLUSIONS

This paper presents a practical approach by addressing a series of experiments to analyze and compare the performance of different active components. It starts with analyzing the PWM generator module from the primary and continues with the field-effect transistors and rectifier diodes in the secondary. The asynchronous flyback topology has been chosen to carry out the experiments. Based on the results obtained, behavioral differences between the components were analyzed using the same experimental platform. The areas of applicability of the performed experiments aim at using active circuit components in the case of power supplies with flyback topology, and in particular, the type of component for power supplies that do not exceed the delivered power of 50 W.

Future research directions are needed in the field of power supplies using flyback topology in both synchronous and asynchronous modes.

ACKNOWLEDGMENTS

The results presented in this article have been funded by the Ministry of Investments and European Projects through the Human Capital Sectoral Operational Program 2014-2020, Contract no. 62461/03.06.2022, SMIS code 153735.

Received on 15 February 2024

REFERENCES

1. K. Sasikala, R. Kumar, *An improved power factor correction for interleaved flyback switched mode power supply*, International Journal of Engineering and Technology (UAE), **7,** *3.27*, pp. 166–169 (2018).
2. A. A. Tulbure, D. Turschner, M. Abrudean, E. Ceuca, R. Ormenisan, *Experimental comparison of switching with IGBT and MOSFET*, International Conference on Automation, Quality and Testing, Robotics, Cluj-Napoca, Romania, pp. 1–5 (2010).
3. L. Dulau, S. Pontarollo, A. Boimond, J.-F. Garnier, N. Giraudo, O. Terrasse, *A new gate driver integrated circuit for IGBT devices with advanced protections*, IEEE Transactions on Power Electronics, **21**, *1*, pp. 38–44 (2006).
4. E. Wilson, Z. Zhiliang, L. Yan-Fei, P. C. Sen, *A current source gate driver achieving switching loss savings and gate energy recovery at 1-MHz*, IEEE Transactions on Power Electronics, **23**, *2*, pp. 678–691 (2008).
5. M. Adamowicz, S. Giziewski, P. Jędrzej, K. Zbigniew, *Performance comparison of SiC Schottky diodes and silicon ultra-fast recovery diodes*, International Conference-Workshop Compatibility and Power Electronics (CPE), Talin, Estonia, pp. 144–149 (2011).
6. M. Grib, M. Iordache, A. Grib, H.-S. Popescu, O. Laudatu, M. Staniloiu, *The use of Thévenin, Norton and hybrid equivalent circuits in the analysis and polarization of nonlinear analog circuits,* 12th International Conference and Exposition on Electrical and Power Engineering (EPE), Iasi, Romania, pp. 198–207 (2022).
7. D. Niculae, M. Iordache, M.-L. Bobaru, M. Stanculescu, O. Drosu, A. Moscu, *Dedicated analog circuit simulation programs*, 14th The International Conference on Electromechanical and Energy Systems SIELMEN, Chișinău, Moldova, pp. 1–6 (2023).
8. M. Iordache, M. Stanculescu, A. Pau, M.-L. Bobaru, H. Andrei, E. Diaconu, C. Cobianu, I. Caciula, D. Niculae, *Equivalent models of nonlinear circuit elements in non sinusoidal regime,* The 10th International Conference on Modern Power Systems MPS, Cluj-Napoca, Romania, pp. 1–5 (2023).
9. O.-D. Laudatu, M. Iordache, *Comparison of inductive and capacitive couplings used to close the feedback loop used in switch mode power supplies*, Rev. Roum. Sci. Techn. – Électrotechn. et Énerg., **68**, *4*, pp. 363–368 (2023).